Online ISSN 1848-3380, Print ISSN 0005-1144
ATKAFF 55(2), 143–152(2014)

Ching-Tang Hsieh, Shu-Han Liao, Chien-Ching Chiu, Min-Hui Ho

Capacity Analysis of MIMO-WLAN Systems with Single Co-Channel Interference

DOI 10.7305/automatika.2014.01.314
UDK 004.73:621.396.6; 519.724
IFAC 2.8.3; 5.8; 1.1.6

Original scientific paper

In this paper, channel capacity of multiple-input multiple-output wireless local area network (MIMO-WLAN) systems with single co-channel interference (CCI) is calculated. A ray-tracing approach is used to calculate the channel frequency response, which is further used to calculate the corresponding channel capacity. The ability to combat CCI for the MIMO-WLAN simple uniform linear array (ULA) and polarization diversity array (PDA) are investigated. Also the effects caused by two antenna arrays for desired system and CCI are quantified. Numerical results show that MIMO-PDA is better than those of MIMO-ULA when interference is present.

Key words: MIMO-WLAN, Single CCI, Ray-tracing Approach, Channel Capacity

Analiza kapaciteta MIMO WLAN sustava s jednom istokanalnom interferencijom. U ovom radu je izračunat kapacitet kanala bežične lokalne računalne mreže s više ulaza i više izlaza te jednom istokanalnom interferencijom. Pristup praćenja zrake je korišten za proračun frekvencijskog odziva kanala iz kojega je potom dobiven njegov kapacitet. Za svladavanje istokanalne interferencije za više-ulazno više-izlaznu bežičnu lokalnu računalnu mrežu istražena je mogućnost korištenja jednostavnog jednoliko raspoređenog polja i polja s polarizacijskom različitosti. Također su kvantificirani efekti prouzročeni dvama poljima antena za razmatrani sustav i istokanalnom interferencijom. Numerički rezultati pokazuju kako je polje s polarizacijskom različitosti bolji izbor od jednoliko raspoređenog polja, uz prisutnu interferenciju.

Ključne riječi: više-ulazno više-izlazna bežična lokalna računalna mreža, istokanalna interferencija, pristup praćenja zrake, kapacitet kanala

1 INTRODUCTION

In recent years there has been a growing interest in the development of potentially mass-producible application systems using millimeter waves, such as wireless LAN (local area networks) systems [1]. To develop millimeter-wave wireless LAN systems, however, we need to know the reflection and transmission characteristics in millimeter-wave bands so that we can evaluate indoor multipath propagation characteristics and the interactions of millimeter waves with various objects.

This paper addresses basic issues regarding the wireless LAN systems that operate in the 60 GHz band as part of the fourth-generation system [2]. The 60 GHz band provides 7 GHz of unlicensed spectrum with a potential to develop wireless communication systems with multi Gbps throughput. The IEEE 802.11 standard committee [3], one of the major organizations in WLAN specifications development, established the IEEE 802.11ad task group to develop an amendment for the 60 GHz WLAN systems.

For wireless communication systems, two main sources of performance degradation are the thermal noise present in the channel or generated in the receiver and unwanted signals emanating from the same or nearby stations. CCI is one of the unwanted signals and it appears due to frequency reuse in wireless channels. CCI reduction has been studied and used in a very limited form in wireless networks [4]-[6]. The use of directional antennas and antenna arrays has long been recognized as an effective technique for reducing CCI, since the differentiation between the spatial signatures of the desired signal and CCI signals can be exploited to reduce the interference when multiple antennas are used.

In a classical large cellular system, due to several interferers in different co-channel cells, the CCIs can be assumed as statistical random variables. Most studies have been based on this assumption of CCI in MIMO systems [7]-[9]. However, this assumption is not suitable for MIMO-WLAN systems for the following reasons. First, in

a small personal communication system (such as WLAN systems), CCI is probably caused by a few signals from adjacent rooms. Second, the use of adaptive antennas and intelligent channel assignment techniques make the case of a large number of CCIs less probable.

In this paper channel capacity of multiple-input multiple-output ultra-wide band (MIMO-WLAN) systems with single CCI is calculated at the 60GHz band. Simple uniform linear array and polarization diversity array are applied to the desired system and the CCI respectively to observe the effects caused by the two antenna arrays. The remainder of this paper is organized as follows. In Section 2, system description and channel modeling are presented. Several numerical results are given in Section 3. Section 4 concludes the paper.

2 SYSTEM DESCRIPTION AND CHANNEL MODELING

2.1 System description

A time-invariant narrowband MIMO system with CCI can be described as follows:

$$\mathbf{Y} = \mathbf{H_d X_d} + \mathbf{H_i X_i} + \mathbf{W} \tag{1}$$

where $\mathbf{Y}$, $\mathbf{X_d}$, $\mathbf{X_i}$ and $\mathbf{W}$ denote the $N_r \times 1$ received signal vector, the $N_t \times 1$ desired transmitted signal vector, the $N_i \times 1$ interference signal vector and the $N_r \times 1$ zero mean additive white Gaussian noise vector at the symbol time, respectively. In (1), $\mathbf{H_d}$ is the $N_r \times N_t$ channel matrix for the desired signal, and the element h_{xy} of the channel matrix $\mathbf{H_d}$ denotes the complex channel gain from the *y*-th transmitting antenna to the *x*-th receiving antenna, $\mathbf{H_i}$ is the $N_r \times N_i$ channel matrix for interference signal, and the element h_{xi} of the channel matrix $\mathbf{H_i}$ denotes the complex channel gain from the i-th interference antenna to the x-th receiving antenna.

A matrix representation of the system is shown in Figure 1. In this figure, the desired signal can be fed into several uncorrelated sub-channels by SVD (Singular Value Decomposition) of the channel matrix $\mathbf{H_d}$and the corresponding signal processing [4], [5]. However, the signal processing and SVD is useless for the interference signal, since the interference channel matrix $\mathbf{H_i}$ is unknown to the receiver. As a result, the received signal can be expressed as follows:

$$\hat{\mathbf{Y}} = \hat{\mathbf{U}}(\mathbf{UDV}^*)\hat{\mathbf{V}}\mathbf{X_d} + \hat{\mathbf{U}}\mathbf{H_i X_i} + \hat{\mathbf{U}}\mathbf{W} \tag{2}$$

where $\mathbf{U}$ and $\mathbf{V}^*$ are the $N_r \times N_r$ and $N_t \times N_t$ unitary matrices, $\mathbf{D}$ is a $N_r \times N_t$ rectangular matrix whose diagonal elements are non-negative real values and other elements are zero, $\hat{\mathbf{V}}$ and $\hat{\mathbf{U}}$ are linear signal processing operation. If channel state information (CSI) is known at both transmitting side and receiving side, the processing operations, $\hat{\mathbf{V}}$ and $\hat{\mathbf{U}}$, can be expressed as $\mathbf{V}$ and $\mathbf{U}^*$, respectively. Then, equation (2) can be rewritten as follows:

$$\hat{\mathbf{Y}} = \mathbf{DX_d} + \mathbf{SX_i} + \hat{\mathbf{W}} \tag{3}$$

where $\mathbf{S} = \mathbf{U}^*\mathbf{H_i}$ denotes a $N_r \times N_i$ equivalent channel matrix for the interference, $\hat{\mathbf{W}} = \mathbf{U}^*\mathbf{W}$ is still a zero mean additive white Gaussian noise vector.

Channel capacity of the system with full CSI can be expressed as follows:

$$C_f^{NB} = B\sum_{x=1}^{N_m} \log_2\left(1 + \frac{P_{d,x} \times \lambda_x}{\sum_{y=1}^{N_i}\left(P_{i,y} \times s_{x,y}^2\right) + P_{n,x}}\right) \tag{4}$$

where f and B are the frequency index and the bandwidth of the system, respectively, $P_{d,x}$ is the power of desired signal transmitted into the x-th sub-channel, $P_{n,x}$ is the power of zero mean additive white Gaussian noise in the x-th sub-channel, $P_{i,y}$ is the power transmitted by the y-th interference antenna, λ_x is the channel power gain of the x-th sub-channel for the desired signal, $s_{x,y}^2$ is the squared value of the matrix S corresponding to the x-th row and the *y*-th column, and N_m is defined as $\min(N_t, N_r)$. If the transmitter of the desired signal has excited each separate channel with equal power, and each interference antenna has also excited with equal power by the transmitter of the interference signal, equation (4) can be rewritten as

$$C_f^{NB} = B\sum_{x=1}^{N_m} \log_2\left(1 + \frac{\frac{P_d}{N_m} \times \lambda_x}{\frac{P_i}{N_i}\sum_{y=1}^{N_i} s_{x,y}^2 + P_{n,x}}\right) \tag{5}$$

where P_d and P_i are the total transmitting powers of the desired signal and the interference signal, respectively.

The equation can be modified further by the following steps. First, the right term both in numerator and denominator inside the parentheses is divided by the noise power $P_{n,x}$, and the equation can be rewritten as follows:

$$C_f^{NB} = B\sum_{x=1}^{N_m} \log_2\left(1 + \frac{\frac{P_d}{N_m \times P_{n,x}} \times \lambda_x}{\frac{P_i}{N_i \times P_{n,x}}\sum_{y=1}^{N_i} s_{x,y}^2 + 1}\right) \tag{6}$$

Then, P_i is multiplied by $\frac{P_d}{P_d}$, and the equation can be rewritten again as follows:

$$C_f^{NB} = B\sum_{x=1}^{N_m} \log_2\left(1 + \frac{\frac{P_d}{N_m \times P_{n,x}} \times \lambda_x}{\frac{P_i \times P_d}{N_i \times P_{n,x} \times P_d}\sum_{y=1}^{N_i} s_{x,y}^2 + 1}\right) \tag{7}$$

Finally, the equation can be organized as follows:

$$C_f^{NB} = B\sum_{x=1}^{N_m} \log_2\left(1 + \frac{\frac{SNRt}{N_m} \times \lambda_x}{\frac{SNRt \times ISR}{N_i}\sum_{y=1}^{N_i} s_{x,y}^2 + 1}\right) \tag{8}$$

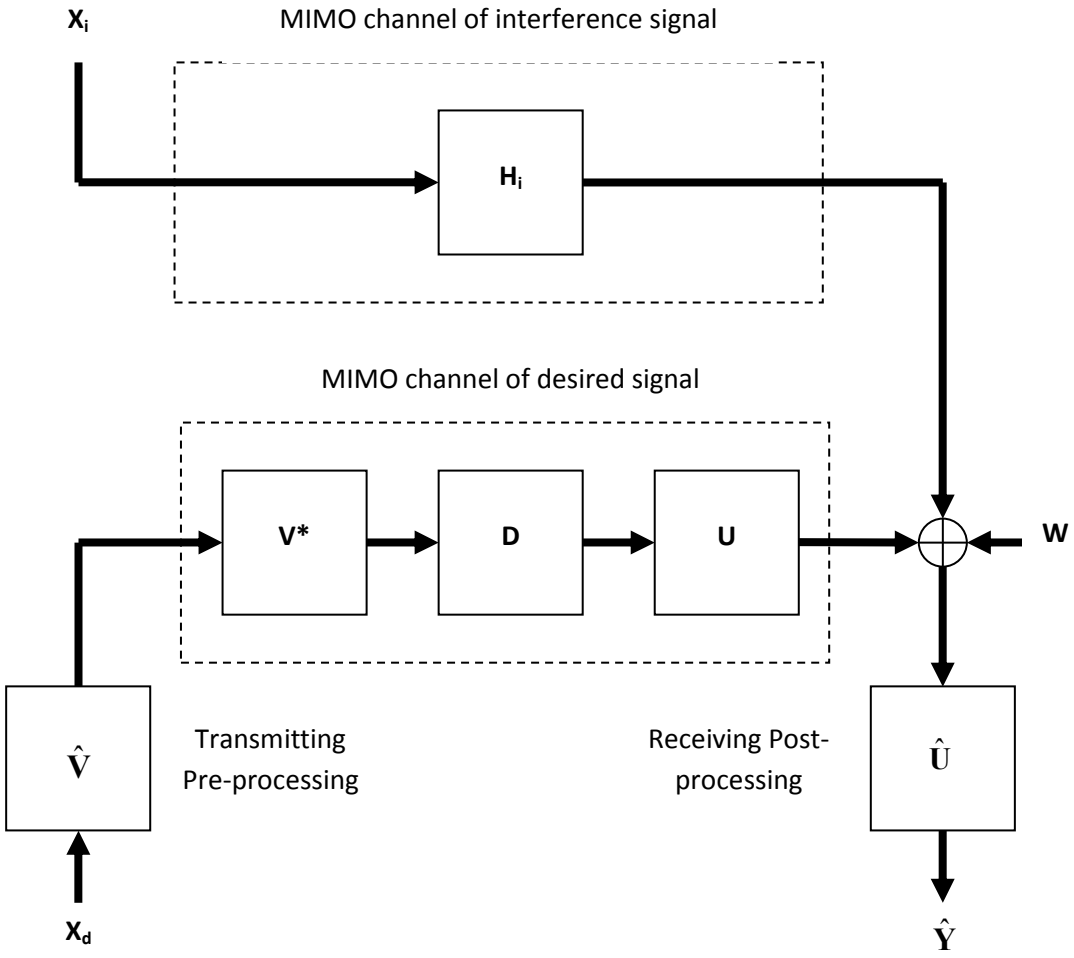

Fig. 1. A matrix representation of MIMO-NB system with single CCI

where *SNRt* denotes the ratio of the total transmitting power of the desired signal to noise power of the receiver and ISR is the ratio of the total transmitting power of the interference signal to that of the desired signal. Note that $ISR = 1$ is considered through this paper to assume that the total transmitting power of desire

2.2 Channel modelling

The shooting and bouncing ray/image (SBR/Image) [10-32] method can deal with high frequency radio wave propagation in the complex indoor environments [33], [34]. It conceptually assumes that many triangular ray tubes are shot from the transmitting antenna (TX), and each ray tube, bouncing and penetrating in the environments is traced in the indoor multi-path channel. If the receiving antenna (RX) is within a ray tube, the ray tube will have contributions to the received field at the RX, and the corresponding equivalent source (image) can be determined. By summing all contributions of these images, we can obtain the total received field at the RX. In real environment, external noise in the channel propagation has been considered. The depolarization yielded by multiple reflections, refraction and first order diffraction is also taken into account in our simulations. Note that the different values of dielectric constant and conductivity of materials for different frequency are carefully considered in channel modeling.

Using ray-tracing approaches to predict channel characteristic is effective and fast, and the approaches are also usually applied to MIMO channel modeling in recent years [35], [36]. Thus, a ray-tracing channel model is developed to calculate wanted channel matrix of MIMO-WLAN system. Flow chart of the ray-tracing process is shown in Figure 2. It conceptually assumes that many triangular ray tubes (not rays) are shot from a transmitter. Here the triangular ray tubes whose vertexes are on a sphere are de-

termined by the following method. First, we construct an icosahedron which is made of 20 identical equilateral triangles. Then, each triangle of the icosahedron is tessellated into a lot of smaller equilateral triangles. Finally, these small triangles are projected on to the sphere and each ray tube whose vertexes are determined by the small equilateral triangle is constructed [37]. For each ray tube bounc-

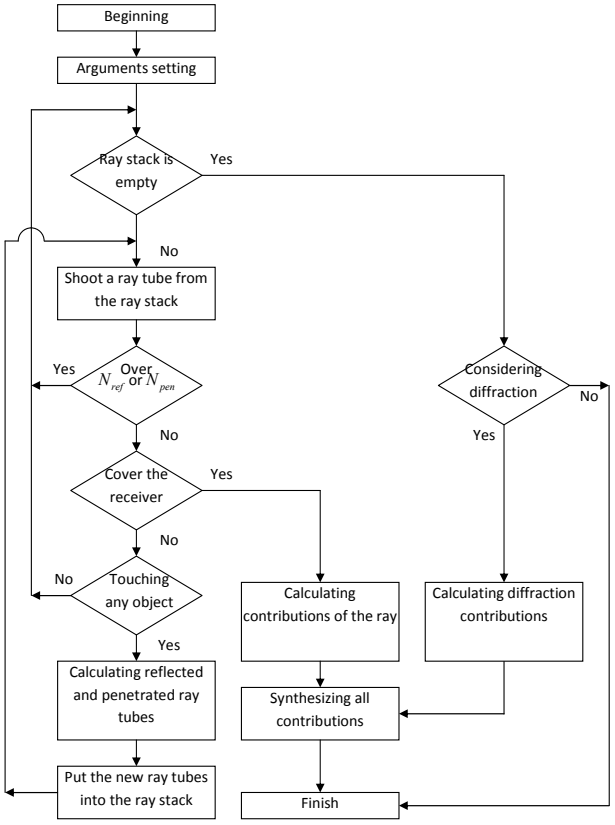

Fig. 2. Flow chart of the ray-tracing process

ing and penetrating in the environments, we check whether reflection times and penetration times of the ray tube are larger than the numbers of maximum reflection N_{ref} and maximum penetration N_{pen}, respectively. If they are not, we check whether the receiver falls within the reflected ray tube. If they are, the contribution of the ray tube to the receiver can be attributed to an equivalent source (i.e. image source). In other words, a specular ray going to receiver exists in this tube and this ray can be thought as launched from an image source. Moreover, the field diffracted from illuminated wedges of the objects in the environment is calculated by uniform theory of diffraction (UTD) [38]. Since the contribution of double diffraction is so small in the analysis, we only take single diffraction into consideration in the paper.

By using these images and received fields, the channel

Table 1. Dielectric properties of concrete materials measured at 60 GHz

MATERIALS	**Relative Permittivity**			
	Real	**Imaginary**	**Conductivity**	**Tan loss**
	ε'	ε''	σ	$\tan\{\delta\}$
Concrete (Ceiling, Walls, Partition, Ground)	6.4954	0.4284	1.43	$6.6 \cdot 10^{-2}$
Wood (Wooden Doors, Wood Tables)	1.5	0.09	$3 \cdot 10^{-1}$	$6 \cdot 10^{-2}$

frequency response can be obtained as following [39]

$$H(f) = \sum_{p=1}^{N_p} a_p(f) e^{j\theta_p(f)} \tag{9}$$

where p is the path index, N_p is the number of paths, f is the frequency of sinusoidal wave, $\theta_p(f)$ is the p-th phase shift and $a_p(f)$ is the p-th receiving magnitude. Note that the channel frequency response of WLAN systems can be calculated by equation (9) in the frequency range of WLAN for both desired signal and interference signal.

3 NUMERICAL RESULTS

Layout of a small personal communication environment is shown in Figure 3. In the figure, dimensions of the two rooms are both 2.5 m (length) $\times$ 4.0 m (width) $\times$ 2.5 m (height), and the partition with dimensions of 0.2 m (thickness) $\times$ 4.0 m (width) $\times$ 2.5 m (height) is between the two rooms. Materials of the ceiling, the walls, the partition and the ground are all concrete block. Furthermore, some furniture is in the rooms, including wooden doors, wood tables and iron cabinets. Sizes of the wooden table and the iron cabinet are 1.5 m (length) $\times$ 0.5 m (width), and heights of the wooden table and the iron cabinet are 1 m and 2 m respectively. The dielectric constant and conductivity of the different materials can be refered in [40]-[43]. The dielectric constant and conductivity of the different materials are shown in Table 1.

The transmitter of desired signal located at $x = 2$ m, $y = 1.5$ m, $z = 1.2$ m and the transmitter of interference signal located at $x = 3.2$ m, $y = 1.5$ m, $z = 1.2$ m are placed in Room1 and Room2, respectively. Moreover, 236 receiving antennas are located on the four wooden tables in Room1 with equal distance of 0.1 m. The antennas of both transmitter and receiver belong to vertically polarization and omni-directional dipole antenna for SISO. The elements for the ULA and PDA antennas are dipole antenna. The elements for the ULA are with simple omni-directional radiation pattern and vertically polarized. Fur-

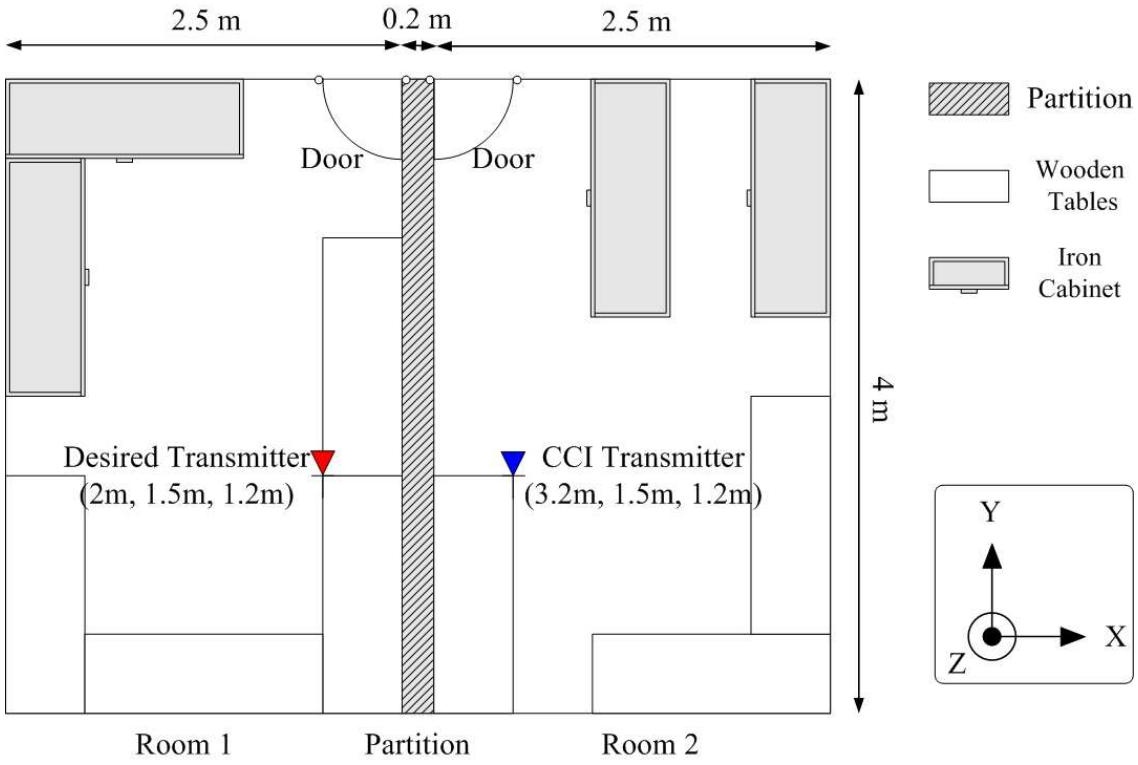

Fig. 3. Layout of a small personal communication environment

thermore, two different antenna arrays, simple uniform linear array (ULA) and polarization diversity array (PDA), are considered as shown in Figure 4(a) and Figure 4(b) respectively.

While the largest wavelength is $\lambda_l = c/f_l \approx 0.005\ m$, where the speed of light, c, is 3×10^8 m/s and the inter-element separation, $d = 0.0025$ m, is chosen to achieve low spatial correlation. Note that strict time stationarity is maintained by ensuring complete physical isolation and absence of any mobile objects.

3.1 Single antenna for the transmitter of CCI

In this paper, the average capacity versus *SNRt* for the MIMO-WLAN simple uniform linear array (ULA) and polarization diversity array (PDA) is calculated. Here channel capacity is the average information rate over the ensemble of channel realizations. There are 236 receiving points for four wooden tables in Room1. In truth, the capacity in equation (8) can be calculated by equal transmitting powers for both MIMO-ULA and MIMO-PDA cases. *SNRt* is the ratio of total transmitting power to noise power for 236 receiving points. As a result, the channel realizations for various receiving locations are combined into one ensemble with 236 samples.

In other words, we have calculated the SNR in all receiving positions. Capacity using that SNR is computed in Fig. 5. The average capacities of WLAN systems calculated from 236 receiving locations for both MIMO-ULA and MIMO-PDA with and without single CCI are shown in Figure 5. It is seen that the capacities without single CCI for simple uniform linear array MIMO (MIMO-ULA) are larger than that for polarization diversity array MIMO (MIMO-PDA). This is due to the fact that MIMO-ULA exhibits approximately equal sub-channel power gain. However, the capacity with single CCI for MIMO-ULA is smaller than that for MIMO-PDA when *SNRt* is large enough, and the opposite results can be seen when *SNRt* is small. The reason is that when MIMO-ULA uses simple uniform linear array to break a multipath channel into several individual spatial channels to enhance capacity, these individual spatial channels also import extra interference power at the moment. In contrast to MIMO-ULA, MIMO-PDA uses tri-polar array to enhance capacity, implying that the interference power is reduced when polarizations of the receiving antenna and interference antenna are not the same. It can be also explained by the fact that the ISR in equation (8) for the MIMO-PDA is smaller than that for the MIMO-ULA. In other words, when MIMO-PDA system breaks a multipath channel into several individual spatial channels to enhance capacity, not all individual spatial channels are affected by interference. A parameter is de-

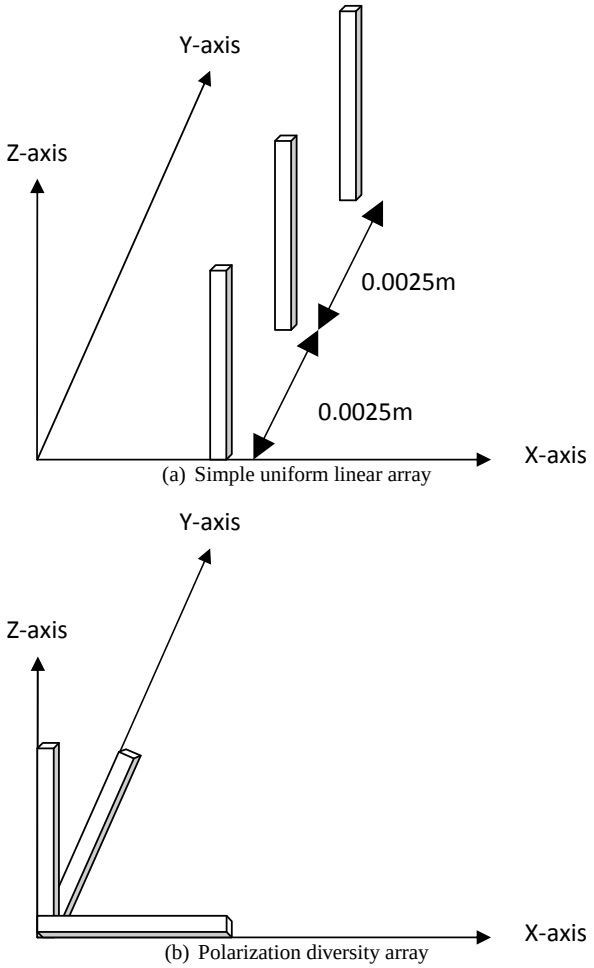

Fig. 4. Layouts of simple uniform linear array and polarization diversity array

fined to check whether MIMO compared to SISO can be used to reduce degradation of capacity while single CCI exist, and it is expressed as

$$VR_c = \frac{\text{Average capatity with single CCI}}{\text{Average capacity without single CCI}} \times 100\% \tag{10}$$

The more the value of VR_c increases, the more degradation of capacity is reduced. In other words, larger VR_c can yield more channel capacity while CCI exist. VR_c for MIMO-ULA, MIMO-PDA and SISO are shown in Figure 6. It is seen that MIMO-PDA can effectively reduce the effect of CCI but MIMO-ULA can not. The results given in Figure 6 are the same as those given in Figure 5. It was found that MIMO-ULA has higher capacity than MIMO-PDA when CCI does not exist. However, MIMO-ULA is not the best choice when single CCI exist, since it can not reduce the degradation of capacity caused by the CCI. In contrast to MIMO-ULA, MIMO-PDA can be used to reduce the degradation of capacity even though it provides less capacity compared to MIMO-ULA when CCI does not exist.

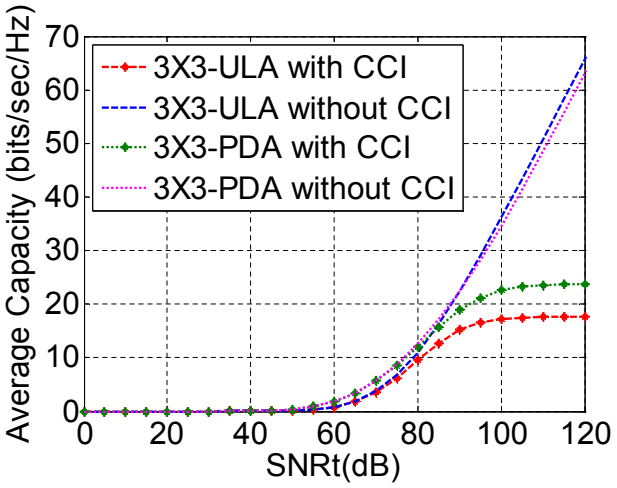

Fig. 5. The average capacities of WLAN systems for both MIMO-ULA and MIMO-PDA with and without single CCI

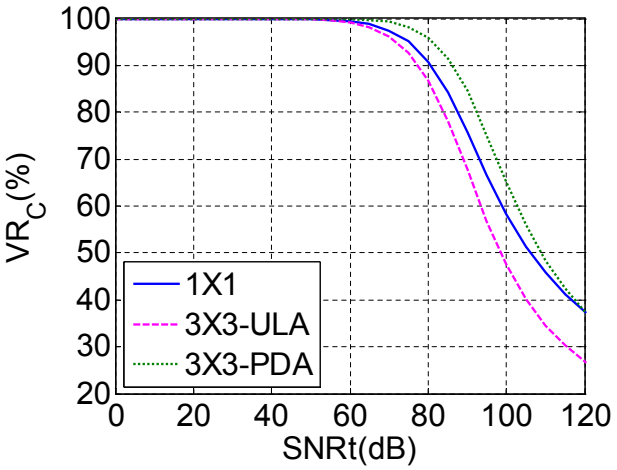

Fig. 6. VR_c for SISO, MIMO-ULA and MIMO-PDA

3.2 Multiple antennas for the transmitter of CCI

The average capacities of WLAN systems calculated from 236 receiving locations with CCI-ULA, CCI-PDA and without CCI for MIMO-ULA and MIMO-PDA are shown in Figure 7 and Figure 8 respectively. Note that the CCI-ULA and the CCI-PDA denote the CCI with simple uniform linear array and polarization diversity array, respectively. In the two figures, the capacity for MIMO-ULA with CCI-PDA is larger than that with CCI-ULA, and the capacity for MIMO-PDA with CCI-ULA is larger than that with CCI-PDA, when *SNRt* is large enough. This is due to that the received CCI power becomes large when

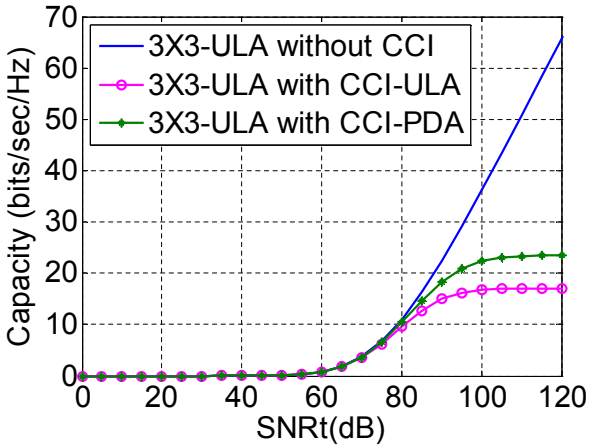

Fig. 7. The average capacities of WLAN systems for MIMO-ULA with CCI-ULA, CCI-PDA and without CCI

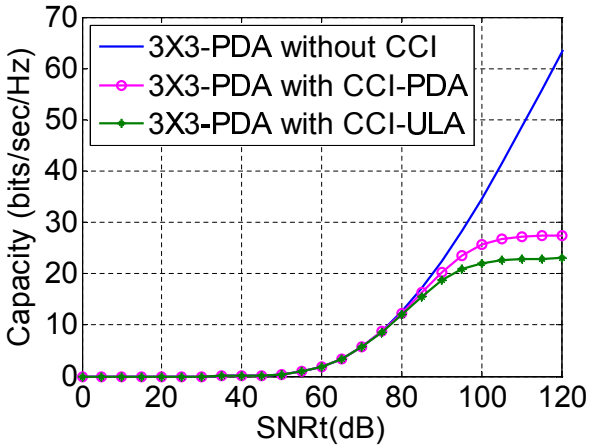

Fig. 8. The average capacities of WLAN systems for MIMO-PDA with CCI-PDA, CCI-ULA and without CCI

antenna arrays of desired system and CCI are the same, and the opposite results can be obtained when antenna arrays of desired system and CCI are different. The same results can also be observed in Figure 9, where the values of VR_c for both MIMO-ULA and MIMO-PDA with CCI-ULA and CCI-PDA are shown. It is concluded that the immunity against CCI for MIMO-PDA is better than that for MIMO-ULA, and the immunity will increase when antenna arrays of the desired system and CCI are different.

4 CONCLUSION

The analyses of the MIMO capacity of WLAN systems with single CCI at 60GHz band have been investigated. Moreover, simple uniform linear array and polarization diversity array are both considered. By the ray-tracing channel model, the average capacities of the MIMO-WLAN

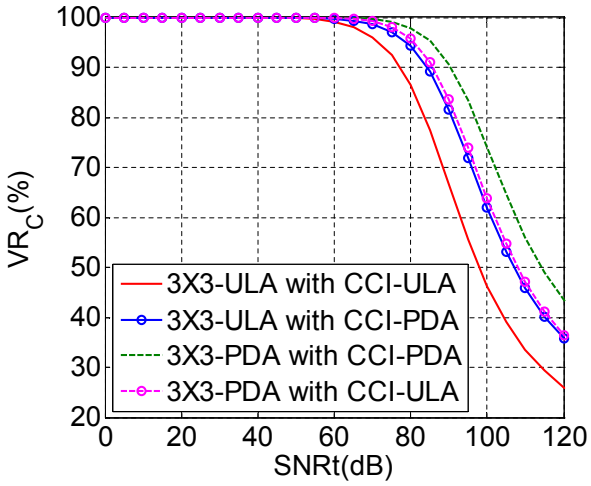

Fig. 9. The average capacities of WLAN systems for MIMO-PDA with CCI-PDA, CCI-ULA and without CCI

system with and without single CCI are calculated for both single and multiple transmitting antennas of the CCI simple uniform linear array and polarization diversity array.

Numerical results show that MIMO-PDA provides somewhat lower gain in SNR and capacity than MIMO-ULA for the interference free case, but offers a feasible alternative for miniaturized WLAN devices owing to its compact, collocated antenna structure, and it keeps a good immunity against the CCI. Moreover, the immunity against CCI for MIMO-PDA is better than that for MIMO-ULA, and the immunity will increase when antenna arrays of the desired system and CCI are different.

REFERENCES

[1] K. Sato, T. Ihara, H. Saito, T. Tanaka, K. Sugai, N. Ohmi, Y. Murakami, M. Shibayama, Y. Konishi and T. Kimura, "Measurements of Reflection and Transmission Characteristics of Interior Structures of Office Buildings in the 60 GHz Band, *IEEE Transactions on Antennas and Propagation*, vol. 45, no. 12, Dec. 1997, pp. 1783-1792.

[2] P. Smulders, "Exploiting the 60 GHz Band for Local Wireless Multimedia Access:Prospects and Future Directions," *IEEE Communications Magazine*, vol. 40, no. 1, Jan. 2002, pp. 140-147.

[3] IEEE Standard for Information Technology - Telecommunications and Information Exchange between Systems - Local and Metropolitan Area Networks - Specific Requirements - *Part 11: Wireless LAN Medium Access Control (MAC) and Physical Layer (PHY) Specifications* – 2007.IEEE Standard 802.11-2007.

[4] G. D. Durgin, *Space-Time Wireless Channels*. New Jersey: Prentice Hall PTR, 2003.

[5] D. Tse and P. Viswanath, *Fundamentals of Wireless Communication*. United Kingdom: Cambridge University Press, 2005.

[6] A. J. Paulraj, R. Nabar and D. Gore, *Introduction to Space-Time Wireless Communication.* U.K.: Cambridge Univ. Press, 2003.

[7] M. Kang, L. Yang, and M. S. Alouini, "Capacity of MIMO Rician Channels with Multiple Correlated Rayleigh Co-Channel Interferers," *IEEE Global Telecommunications Conf.*, Dec. 2003, vol. 2, pp. 1119-1123.

[8] M. Chiani, M. Z. Win and H. Shin, "Capacity of MIMO Systems in the Presence of Interference," *IEEE Global Telecommunications Conf.*, Dec. 2006, pp. 1-6.

[9] M. G. D. Benedetto and G. Giancola, *Understanding Ultra Wide Band Radio Fundamentals*. New Jersey: Prentice Hall PTR, 2004.

[10] C. L. Liu, M. H. Ho, C. C. Chiu and C. Y. Cheng, "A Comparison of UWB Communication Characteristics for Various Corridors," *ACTA International Journal of Modelling and Simulation*, vol. 30, no. 2, May. 2010, pp. 172–177.

[11] S. H. Liao, C. C. Chiu and M. H. Ho "Location Optimization for Antennas by Asynchronous Particle Swarm Optimization" *IET Communications*, Vol. 7, Issue: 14, pp.1510-1516, Sept. 2013.

[12] S. H. Liao, C. H. Chen, C. C. Chiu, M. H. Ho, T. A. Wysocki and B. J. Wysocki "Optimal Receiver Antenna Location in Indoor Environment Using Dynamic Differential Evolution and Genetic Algorithm," *EURASIP Journal on Wireless Communications and Networking*, 235, Sept. 2013.

[13] C. C. Chiu, C. L. Liu and S. H. Liao, "Channel Characteristics of Ultra Wideband Systems with Single Co-Channel Interference," *Wireless Communications and Mobile Computing*, vol. 13, issue 9, pp. 864-873, Jun. 2013.

[14] C. C. Chiu, C. Y. Yu, S. H. Liao and M. K. Wu "Channel Capacity of Multiple-Input Multiple-Output Systems for Optimal Antenna Spacing by Particle Swarm Optimizer," *Wireless Personal Communications*, vol. 69, issue 4, pp. 1865–1876, Apr. 2013.

[15] C. C. Chiu, C. H. Chen, S. H. Liao and K. C. Chen, "Bit Error Rate Reduction by Smart UWB Antenna Array in Indoor Wireless Communication," *Journal of Applied Science and Engineering*, vol. 15, no.2, pp. 139-148, Jun. 2012.

[16] C. C. Chiu, C. H. Chen, S. H. Liao and T. C. Tu, "Ultra-wideband Outdoor Communication Characteristics with and without Traffic," *EURASIP Journal on Wireless Communications and Networking*, 92, Mar. 2012.

[17] C. C. Chiu, Y. T. Kao, S. H. Liao and Y. F. Huang, "'UWB Communication Characteristics for Different Materials and Shapes of the Stairs," *Journal of Communications*, vol. 6, no.8, pp. 628-632, Nov. 2011.

[18] S. H. Liao, H. P. Chen, C. C. Chiu, and C. L. Liu "Channel Capacities of Indoor MIMO-UWB Transmission for Different Material Partitions," *Tamkang Journal of Science and Engineering*, vol. 14, no.1, pp. 49-63, Mar. 2011.

[19] C. L. Liu, C. C. Chiu, S. H. Liao and Y. S. Chen, "Impact of Metallic Furniture on UWB Channel Statistical Characteristics," *Tamkang Journal of Science and Engineering*, vol. 12, no.3 , pp. 271-278, Sept. 2009.

[20] S. H. Liao, C. C. Chiu and M. H. Ho, "Comparison of Dynamic Differential Evolution and Genetic Algorithm for MIMO-WLAN Transmitter Antenna Location in Indoor Environment," *Wireless Personal Communications*, vol. 71, issue 4, pp. 2677–2691, Jul. 2013.

[21] C. C. Chiu, M. H. Ho and S. H. Liao, "MIMO-UWB Smart Antenna Communication Characteristics for Different Antenna Arrays of Transmitters," *International Journal of RF and Microwave Computer-Aided Engineering*, vol. 23, no 3, pp. 378-392, May 2013.

[22] C. C. Chiu, M. H. Ho and S. H. Liao, "PSO and APSO for Optimizing Coverage in Indoor UWB Communication System," *International Journal of RF and Microwave Computer-Aided Engineering*, vol. 23, no 3, pp. 300-308, May 2013.

[23] S. H. Liao, C. C. Chiu, C. H. Chen and M. H. Ho, "Channel Characteristics of MIMO-WLAN Communications at 60GHz for Various Corridors," *EURASIP Journal on Wireless Communications and Networking*, 96, Apr. 2013.

[24] M. H. Ho, C. C. Chiu and S. H. Liao "Comparison of Different Antenna Arrays for the BER Reduction in Indoor Wireless Communication," *International Journal of Communication Systems*, vol. 26, issue 2, pp. 161-176, Feb. 2013.

[25] C. H. Sun, C. C. Chiu, M. H. Ho and C. L. Li, "Comparison of Dynamic Differential Evolution and Self–Adaptive Dynamic Differential Evolution for Buried Metallic Cylinder," *Research in Nondestructive Evaluation*, vol. 24, Jan. 2013, pp. 35–50.

[26] M. H. Ho, C. C. Chiu and S. H. Liao, "Optimization of Channel Capacity for MIMO Smart Antenna Using Particle Swarm Optimizer," *IET Communications*, vol. 6, issue 16, Nov. 2012, pp. 2645–2563.

[27] M. H. Ho, C. C. Chiu and S. H. Liao, "Bit Error Rate Reduction for Circular Ultrawideband Antenna by Dynamic Differential Evolution," *International Journal of RF and Microwave Computer–Aided Engineering*, vol. 22, no. 2, Mar. 2012, pp. 260–271.

[28] S. H. Liao, M. H. Ho, C. C. Chiu and C. H. Lin, "Optimal Relay Antenna Location in Indoor Environment Using Particle Swarm Optimizer and Genetic Algorithm," *Wireless Personal Communications*, vol. 62, no. 3, Feb. 2012, pp. 599–615.

[29] S. H. Liao, C. C. Chiu, M. H. Ho and C. L. Liu, "Channel Capacity of Multiple–Input Multiple–Output Ultra Wide Band Systems with Single Co–channel Interference," *International Journal of Communication Systems*, vol. 23, issue 12, Dec. 2010, pp. 1600–1612.

[30] S. H. Liao, M. H. Ho and C. C. Chiu, "Bit Error Rate Reduction for Multiusers by Smart UWB Antenna Array," *Progress In Electromagnetic Research C*, vol. 16. PIER C 16, Sep. 2010, pp. 85–98.

[31] M. H. Ho, S. H. Liao and C. C. Chiu, "UWB Communication Characteristics for Different Distribution of People and Various Materials of Walls," *Tamkang Journal of Science and Engineering*, vol. 13, no.3, Sep. 2010, pp.315–326.

[32] M. H. Ho, S. H. Liao and C. C. Chiu, "A Novel Smart UWB Antenna Array Design by PSO," *Progress In Electromagnetic Research C*, vol. 15. PIER C 15, Aug. 2010, pp. 103–115.

[33] I. Oppermann, M. Hämäläinen and J. Iinatti, *UWB Theory and Applications*. New Jersey: Prentice Hall PTR, 2004.

[34] H. Arslan, Z. N. Chen and M. G. D. Benedetto, *Ultra Wideband Wireless Communication*. New Jersey: John Wiley & Sons, Inc., 2006.

[35] S. Loredo, A. R. Alonso and R. P. Torres, "Indoor MIMO Channel Modeling by Rigorous GO/UTD-Based Ray Tracing," *IEEE Trans. Veh. Technol.*, vol. 57, no. 2, Mar. 2008, pp. 680-692.

[36] W. Q. Malik, C. J. Stevens and D. J. Edwards, "Spatio-Temporal Ultra Wideband Indoor Propagation Modeling by Reduced Complexity Geometric Optics," *IET Commun.*, vol. 1, no. 4, 2007, pp. 751-759.

[37] S. H. Chen and S. K. Jeng, "An SBR/image Approach for Radio Wave Propagation in Indoor Environments with Metallic Furniture," *IEEE Trans. Antennas Propagat.*, vol. 45, no. 1, 1997, pp. 98-106.

[38] C. A. Balanis, *Advanced Engineering Electromagnetics*. USA: John Wiley & Sons Press, 1989.

[39] P. C. Richardson, Weidong Xiang and Wayne Stark, "Modeling of Ultra-Wideband Channels within Vehicles," *IEEE J. Sel. Areas Commun.*, vol. 24, no. 4, 2006, pp. 906-912.

[40] L. M. Correia and P. O. Frangęs, "Estimation of Materials Characteristics from Power Measurements at 60 GHz," *International Symposium on Personal, Indoor and Mobile Radio Communications*, Den Haag (Netherlands), Sep. 1994, pp.510-513.

[41] Y. Pinhasi, A. Yahalom and S. Petnev, "Propagation of Ultra Wide-Band Signals in Lossy Dispersive Media," *IEEE International Conference on Microwaves, Communications, Antennas and Electronic Systems*, COMCAS, May 13-14, 2008, pp.1-10.

[42] V. Pertti, "On the Properties of Dielectric Materials in Mobile Communications Enviroments", *COST 2100 TD*(10)*12097*, Bologna, Italy, Nov. 2010, pp. 23-25.

[43] Y. Lostanlen, Y. Corre, Y. Louet, Y. L. Helloco and S. Collonge, "Comparison of Measurements and Simulations in Indoor Environments for Wireless Local Networks at 60 GHz", *IEEE 55th Vehicular Technology Conference*, vol. 1, 2002, pp. 389-393.

Ching-Tang Hsieh is a Professor of electrical engineering at Tamkang University, Taiwan, R.O.C. He received the B.S. degree in electrical engineering in 1976 from TKU and the M.S. and Ph.D. degrees in 1985 and 1988, respectively, from Tokyo Institute of Technology, Japan. From 1990 to 1996, he acted as the Chairman of the Department of electrical engineering. His current research interests include speaker recognition, fingerprint identification, image inpainting, image processing and fuzzy system.

Shu-Han Liao was born in Taipei, Taiwan, Republic of China, on September 18, 1982. He received the M.S.C.E. degree from Feng Chia University in 2008 and a Ph.D. degree in electrical engineering from Tamkang University, Taipei, Taiwan, in 2013. Currently, he is a Senior Engineer with the Advanced Communication System Center, Smart & Network System Institute, Institute for Information Industry, Taipei. Dr. Liao holds two patents and more than 40 technical papers in international journals and conference proceedings. His current research interests include indoor wireless communication systems, smart antenna, optimization methods, Co-channel interference analysis, relay systems, ultra-wideband systems, next generation (4G/5G) mobile systems, LTE/ LTE-A, Patent and MIMO systems.

Chien-Ching Chiu received his BSCE degree from National Chiao Tung University, Hsinchu, Taiwan, in 1985, and his MSEE and PhD degrees from National Taiwan University, Taipei, in 1987 and 1991, respectively. From 1987 to 1989, he was a communication officer with the ROC Army Force. In 1992, he joined the faculty of the Department of Electrical Engineering, Tamkang University, where he is now a professor. From 1998 to 1999, he was a visiting scholar at the Massachusetts Institute of Technology, Cambridge, and the University of Illinois at Urbana-Champaign. He is a visiting professor with the University of Wollongong, Australia, in 2006. Moreover, he was a visiting professor with the University of London, United Kingdom, in 2011. His current research interests include microwave imaging, numerical techniques in electromagnetics, indoor wireless communications, and ultra-wideband communication systems. He has published more than 110 journal papers on inverse scattering problems, communication systems, and optimization algorithms.

Min-Hui Ho was born in Taipei, Taiwan, Republic of China, on March 30, 1983. She received the MSEE and PhD degrees in electrical engineering from Tamkang University, Taipei, Taiwan, in 2007 and 2013, respectively. Her current research interests include indoor wireless communication systems, smart antenna, MIMO systems, optimization methods, and ultra-wideband systems.

AUTHORS' ADDRESSES
Prof. Ching-Tang Hsieh, Ph.D.
Prof. Chien-Ching Chiu, Ph.D.
Department of electrical engineering,
Tamkang University,
New Taipei City, Taiwan, R.O.C
email: 073063@mail.tku.edu.tw, chiu@ee.tku.edu.tw
Shu-Han Liao, Ph.D.
Advanced Communication System Center,
Smart & Network System Institute,
Institute for Information Industry,
Taipei, Taiwan, R.O.C.
email: shliao@iii.org.tw,
Min-Hui Ho, Ph.D.
Smart & Network System Institute,
Institute for Information Industry,
Taipei, Taiwan, R.O.C.
email:katrina650@hotmail.com

Received: 2012-07-01
Accepted: 2013-05-21